

## Supplementary Material

# Portability of a Small Molecule Binding Site Between Disordered Proteins

Rajesh Jaiprashad, Sachith Roch De Silva, Lisette M. Fred Lucena, Ella Meyer, Steven J. Metallo

## Table of Contents

**Fig S1.** Myc, MaxRH, MaxRH-Y115F/Y123F, P22 Max, and P21 Max constructs aligned using CLUSTAL O (1.2.4) multiple sequence alignment

**Fig S2.** UV/Vis characterization of 34RH

**Fig S3.** Dynamic light scattering of 34RH in 1xPBS (buffer) at pH 7.4

**Fig S4.** Myc<sub>353-437</sub> and 34RH interaction monitored via tyrosine fluorescence quenching and free fluorescence spectra of Myc<sub>353-437</sub> and 34RH

**Fig S5.** Equimolar Myc<sub>353-437</sub> and 34RH interaction monitored via tyrosine fluorescence quenching

**Fig S6.** NMR characterization of 34RH

Myc	-----gsNVKRRTHNVLERQRRNELKRSFFALRDQIPELE	385
MaxRH	-----gMSDNDDIEVESDEEQPRFQSAADKRAHHNALERKRRDH <span style="font-family: monospace;">IKDSFHSLRDSVPSLQ</span>	54
MaxRH*	-----gMSDNDDIEVESDEEQPRFQSAADKRAHHNALERKRRDH <span style="font-family: monospace;">IKDSFHSLRDSVPSLQ</span>	54
P22	gidpf <span style="font-family: monospace;">tMSDNDDIEVESDEEQPRFQSAADKRAHHNALERKRRDH<span style="font-family: monospace;">IKDSFHSLRDSVPSLQ</span></span>	54
P21	gidpf <span style="font-family: monospace;">tMSDNDDIEVESD-----ADKRAHHNALERKRRDH<span style="font-family: monospace;">IKDSFHSLRDSVPSLQ</span></span>	45

\*\* \* \*.\*\*\*:\*\*\*:..: \* \* .:\*\*\*. :\*.\*:

Myc	NNEKAPKVVLKKATAYILSVQAEEQKLISEEDLLRKREQLKH <span style="font-family: monospace;">KLEQL---RNS-----</span>	437
MaxRH	G-EKASRAQILD <span style="font-family: monospace;">KATEYILSVQAENHTHQ<span style="font-family: monospace;">QDIDDLKRQNALLEQQVR<span style="font-family: monospace;">ALEKARSSAQ<span style="font-family: monospace;">LQT</span></span></span></span>	113
MaxRH*	G-EKASRAQILD <span style="font-family: monospace;">KATEYILSVQAENHTHQ<span style="font-family: monospace;">QDIDDLKRQNALLEQQVR<span style="font-family: monospace;">ALEKARSSAQ<span style="font-family: monospace;">LQT</span></span></span></span>	113
P22	G-EKASRAQILD <span style="font-family: monospace;">KATEYI<span style="font-family: monospace;">QYMR<span style="font-family: monospace;">RK<span style="font-family: monospace;">NHTHQ<span style="font-family: monospace;">QDIDDLKRQNALLEQQVR<span style="font-family: monospace;">ALEKARSSAQ<span style="font-family: monospace;">LQT</span></span></span></span></span></span></span>	113
P21	G-EKASRAQILD <span style="font-family: monospace;">KATEYI<span style="font-family: monospace;">QYMR<span style="font-family: monospace;">RK<span style="font-family: monospace;">NHTHQ<span style="font-family: monospace;">QDIDDLKRQNALLEQQVR<span style="font-family: monospace;">ALEKARSSAQ<span style="font-family: monospace;">LQT</span></span></span></span></span></span></span>	104

. \*\*\* :. \*\*.\*\*\* \*\* : : ::.. .: \* \*:::. \*:::.. \* \*.\*

Myc	-----	---
MaxRH	NYPSSDNSLYTNAKGSTISAFDGGS <span style="font-family: monospace;">DSSSEPEEPQSRKKLRMEAS</span>	160
MaxRH*	NFPSSDNSLFTNAKGSTISAFDGGS <span style="font-family: monospace;">DSSSEPEEPQSRKKLRMEAS</span>	160
P22	NYPSSDNSLYTNAKGSTISAFDGGS <span style="font-family: monospace;">DSSSEPEEPQSRKKLRMEAS</span>	160
P21	NYPSSDNSLYTNAKGSTISAFDGGS <span style="font-family: monospace;">DSSSEPEEPQSRKKLRMEAS</span>	151

**Fig S1.** Myc, MaxRH, MaxRH-Y115F/Y123F (denoted as MaxRH\* in figure), P22 Max, and P21 Max constructs aligned using CLUSTAL O (1.2.4) multiple sequence alignment. Lowercase letters denote non-native residues remaining after TEV cleavage [63].

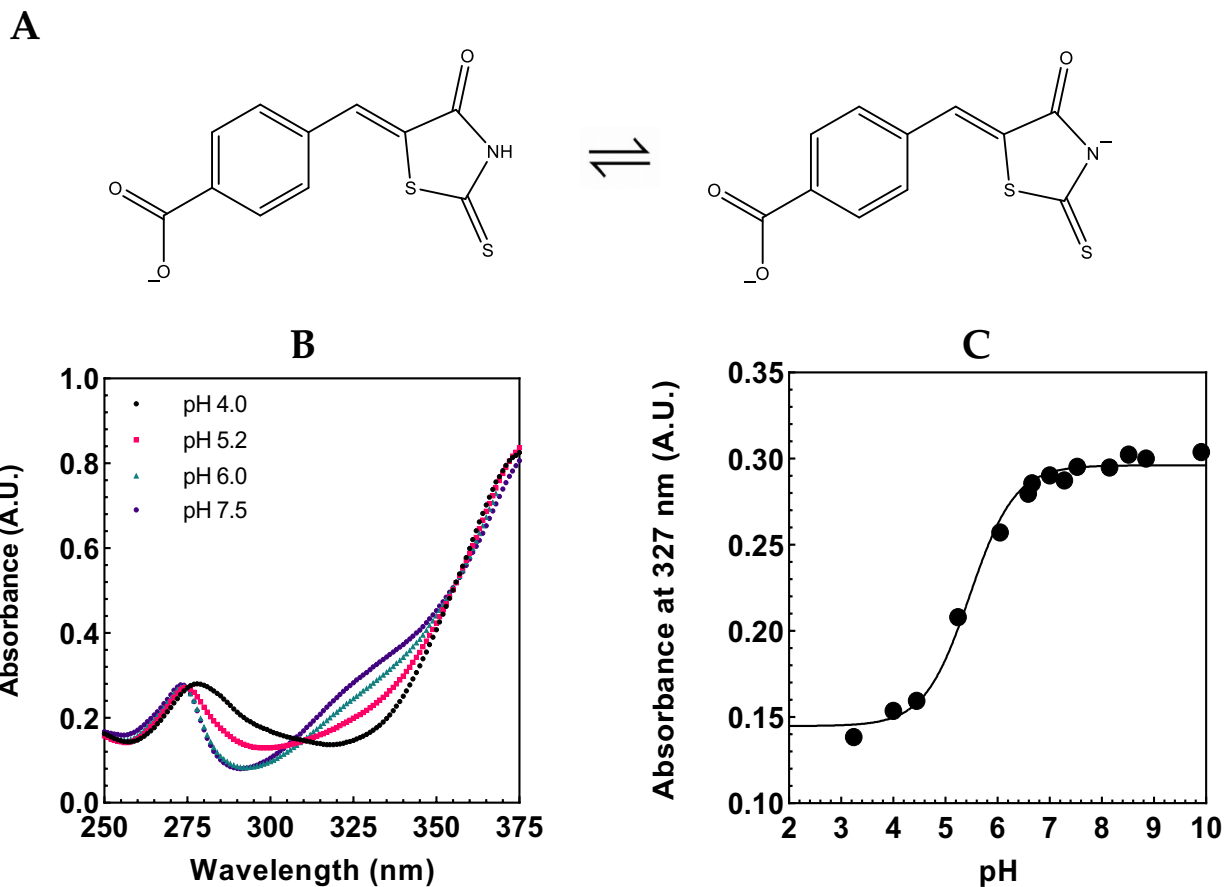


**Fig S2.** UV/Vis characterization of 34RH. (A) pH dependent deprotonation of 34RH. (B) UV/Vis absorbance of 10  $\mu$ M 34RH in 1xPBS, 5% DMSO, 25 °C, at pH 4.0 (black), pH 5.2 (dark pink), pH 6.0 (teal), and pH 7.5 (purple). (C) 34RH absorbance at 327 nm at various pH values showing a pH dependent titration fit to the Henderson-Hasselbalch equation [45].

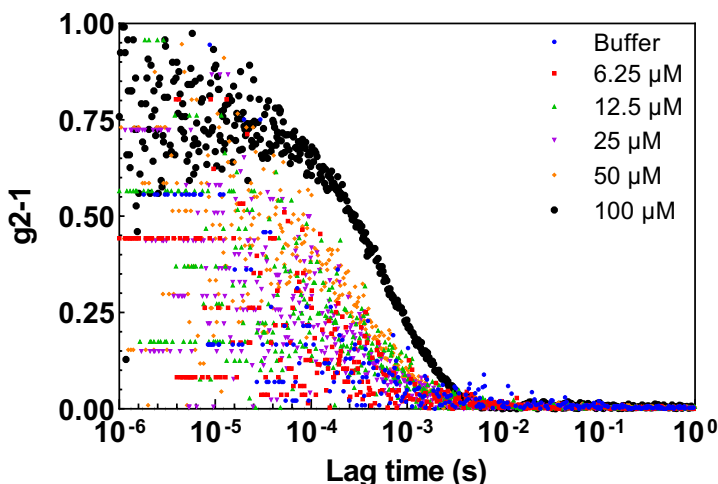


**Fig S3.** Dynamic Light Scattering of 34RH in 1xPBS and 5% DMSO (buffer) at pH 7.4. Concentrations of 34RH are shown in the upper right corner. Concentrations below 50  $\mu$ M show no correlation function indicating that there are none to minimal nano-sized particles in the samples. At 100  $\mu$ M, a correlation was observed indicating that nano-sized particles may exist in solution. All experiments were carried out at 50  $\mu$ M and below to avoid any potential particle interference in the data.

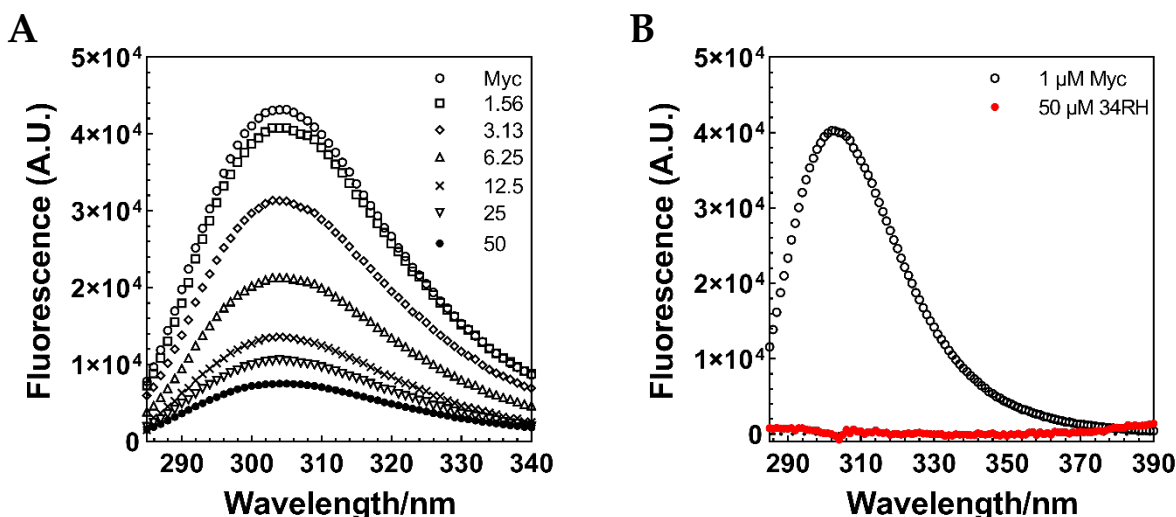


**Fig S4.** Myc<sub>353-437</sub> and 34RH interaction monitored via tyrosine fluorescence quenching and free fluorescence spectra of Myc<sub>353-437</sub> and 34RH. (A) Inner filter corrected fluorescence emission spectra of 1  $\mu$ M Myc<sub>353-437</sub> (open circles) and 1  $\mu$ M Myc<sub>353-437</sub> with various concentrations of 34RH in 1xPBS, 5% DMSO at 25 °C, pH 7.4. Concentrations of 34RH (in micromolar) are shown in the upper right corner. (B) Comparison of inner filter corrected emission spectra of 1  $\mu$ M Myc<sub>353-437</sub> (open circles) and 50  $\mu$ M 34RH without Myc (closed circles) demonstrating no fluorescence contribution from 34RH in this wavelength range.

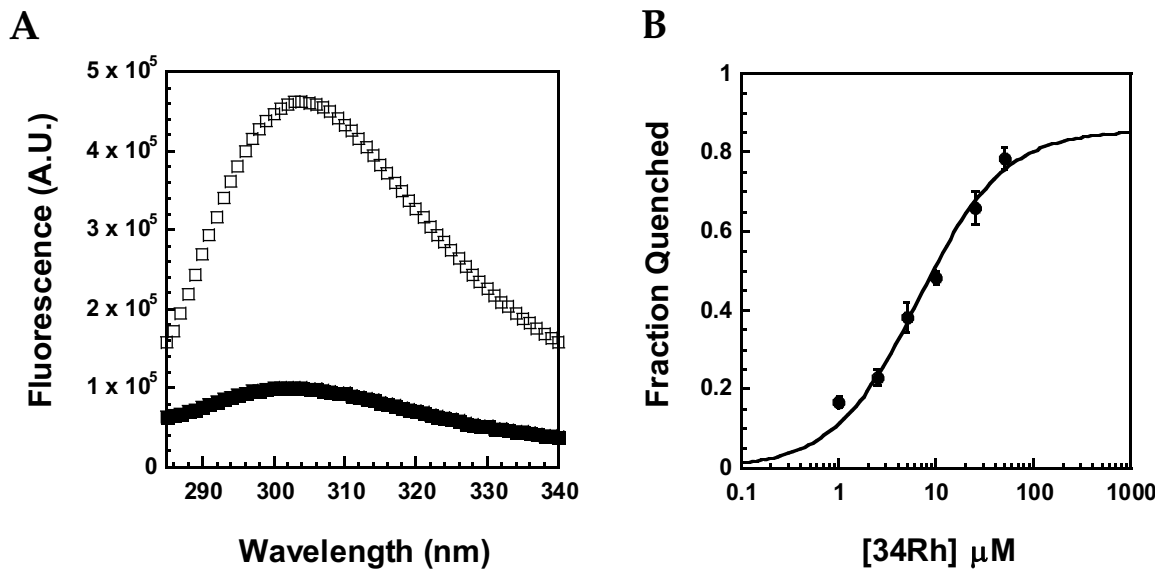


**Fig S5.** Equimolar Myc<sub>353-437</sub> and 34RH interaction monitored via tyrosine fluorescence quenching. **(A)** 50  $\mu\text{M}$  Myc<sub>353-437</sub> in the presence (filled black squares) and absence (open black squares) equimolar 34RH in 1x PBS at 25 °C, pH 7.4. **(B)** Equilibrium quenching of an equimolar titration of Myc<sub>353-437</sub> and 34RH fit to a 1:1 binding model,  $K_D$  of  $5.9 \pm 0.8 \mu\text{M}$ . Error bars represent the standard error of three independent trials. Representative fluorescence signals were inner filter corrected to account for any fluorescence suppression due the absorbance of protein and 34RH [46]. The quenching data was fitted to a binding model shown below described in Dobrev et al.

$$\text{Fraction Quenched} = Q_{\max} \times \frac{2 + \frac{K_D}{[C]_{\text{tot}}} \sqrt{\left(-2 - \frac{K_D}{[C]_{\text{tot}}}\right)^2 - 4}}{2}$$

Here,  $Q_{\max}$  is the fraction quenched for the formation of the complete complex between Myc<sub>353-437</sub> and 34RH.  $[C]_{\text{tot}}$  is the total concentration of Myc<sub>353-437</sub> or 34RH and  $K_D$  the dissociation constant. [46,49]

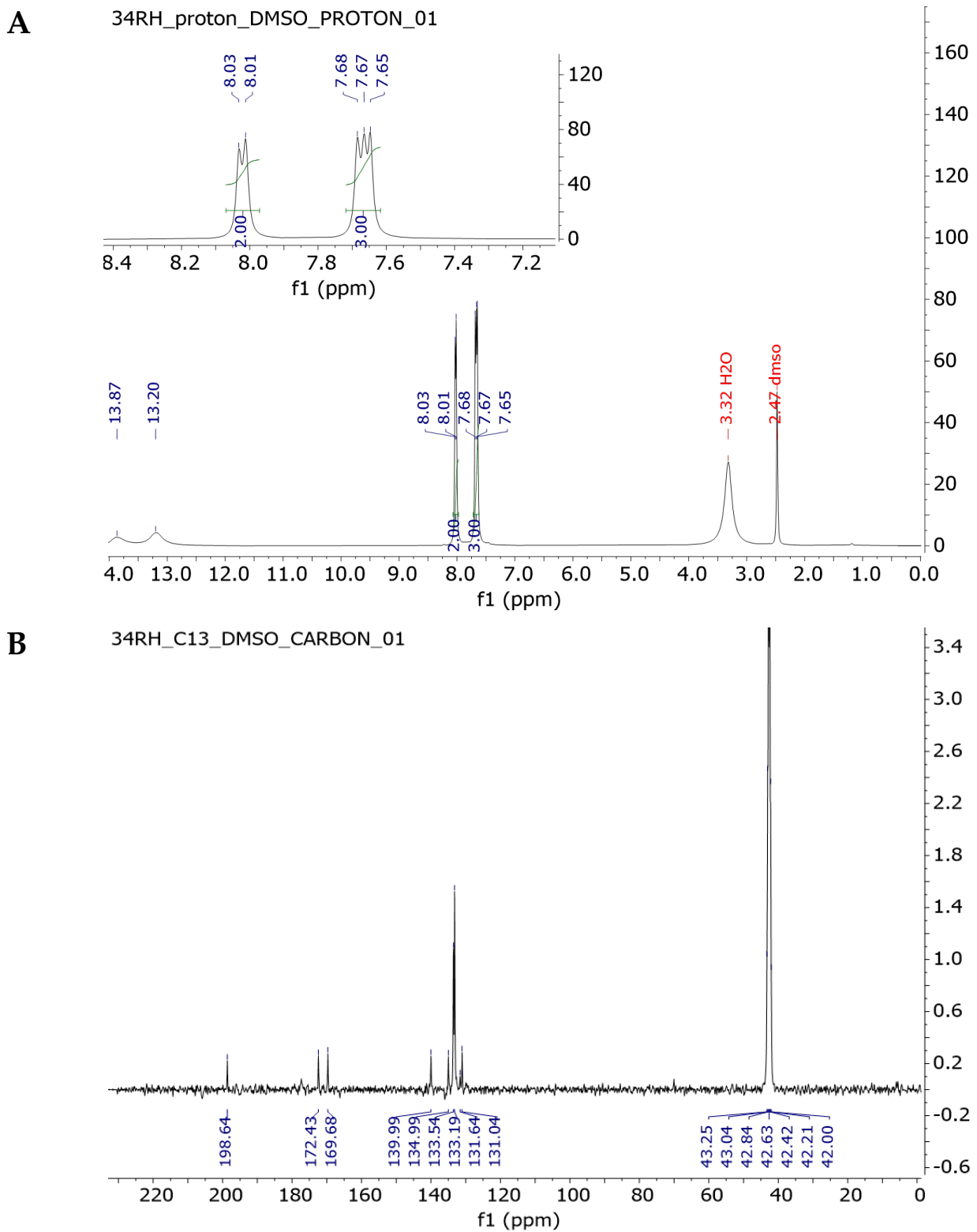


**Fig S6.** NMR characterization of 34RH **A)** 1H NMR of 34RH in DMSO-d<sub>6</sub>. **B)** 13C NMR of 34RH in DMSO-d<sub>6</sub>.

## References

45. Luiz, F.C.L.; Louro, S.R.W. Acid-base equilibrium of drugs in time-resolved fluorescence measurements: Theoretical aspects and expressions for apparent pK(a) shifts. *J Photoch Photobio A* **2011**, *222*, 10-15, doi:10.1016/j.jphotochem.2011.03.006.
46. Dobrev, V. S.; Fred, L. M.; Gerhart, K. P.; Metallo, S. J. *Characterization of the Binding of Small Molecules to Intrinsically Disordered Proteins*, 1st ed.; Elsevier Inc., **2018**; Vol. 611. <https://doi.org/10.1016/bs.mie.2018.09.033>.
49. Follis, A. V.; Hammoudeh, D. I.; Wang, H.; Prochownik, E. V.; Metallo, S. J. Structural Rationale for the Coupled Binding and Unfolding of the C-Myc Oncoprotein by Small Molecules. *Chem. Biol.* **2008**, *15* (11), 1149–1155. <https://doi.org/10.1016/j.chembiol.2008.09.011>.
63. Sievers, F.; Wilm, A.; Dineen, D.; Gibson, T. J.; Karplus, K.; Li, W.; Lopez, R.; McWilliam, H.; Remmert, M.; Söding, J.; et al. Fast, Scalable Generation of High-Quality Protein Multiple Sequence Alignments Using Clustal Omega. *Mol. Syst. Biol.* **2011**, *7* (539). <https://doi.org/10.1038/msb.2011.75>.